Supplementary Matrial

Fermi-Dirac Parameter Optimization

Figure 24, below, illustrates the best regions in the Fermi-Dirac parameter space for successful circle and rectangle reconstructions. These are the scatter plots of one of the two mentioned experiments in Section 4.1. The circle and rectangle geometries were chosen because of their distinct geometrical properties: straight lines vs. curvature, smooth vs. corners. The final reconstruction error was measured which relates to ε_H. Note that the two geometries provide quite different optimal ranges for the Fermi-Dirac parameters T and m (top row). The ranges were identified after combining the results to ensure parameters work well in both scenarios. More and larger experiments have also been carried out with 28 other weighing functions including ten CS-RBF class functions and three SPH smoothing kernels, before optimizing the Fermi-Dirac variant. Here, the best ranges were identified by experiment, and then fine-tuned on the reconstruction examples as well as via error analysis.

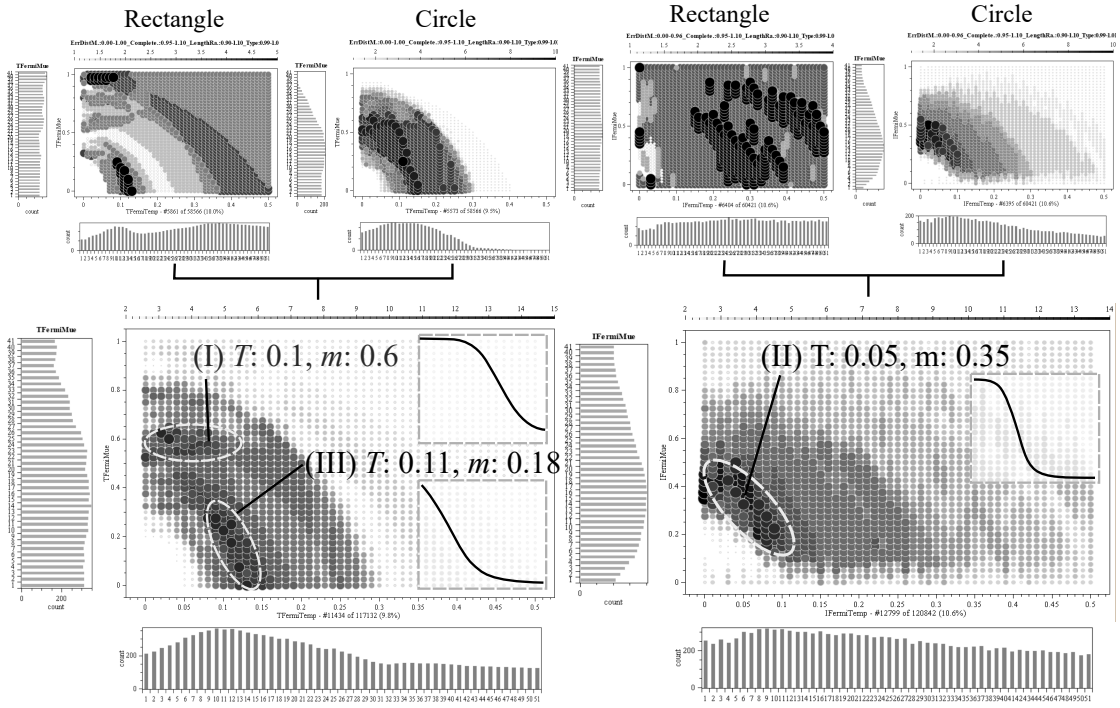

(a) Best for tensor (b) Best for interpolation

Figure 24: The best 10% reconstructions w.r.t. the final reconstruction error illustrated as scatter plots. The Fermi-Dirac parameters T and m were varied (x and y-axis). (Top:) Successes counted for the circle (left) and the rectangle (right) regarding tensor computation (a) and interpolation (b). (Bottom:) Both cases are combined to identify optimal regions of the parameters; here, marked as ellipses. For the tensor computation two regions are found and one for the interpolation. The parameter sets of regions (I) and (II) are utilized throughout all reconstructions, see Equation (2).

Influence of the Covariance Centroid

Dependent on the choice for the centroid c in Equation (1) the covariance and its shape factor yield different results. The variants with a moving center, such as the mean or the geometric median filter noise better. In general, this is beneficial for the integration direction. Figure 25 demonstrates the effect for a very noisy circle set up. Here, a variant of the geometric median is a more robust choice compared to the PDT and MN (PCA).

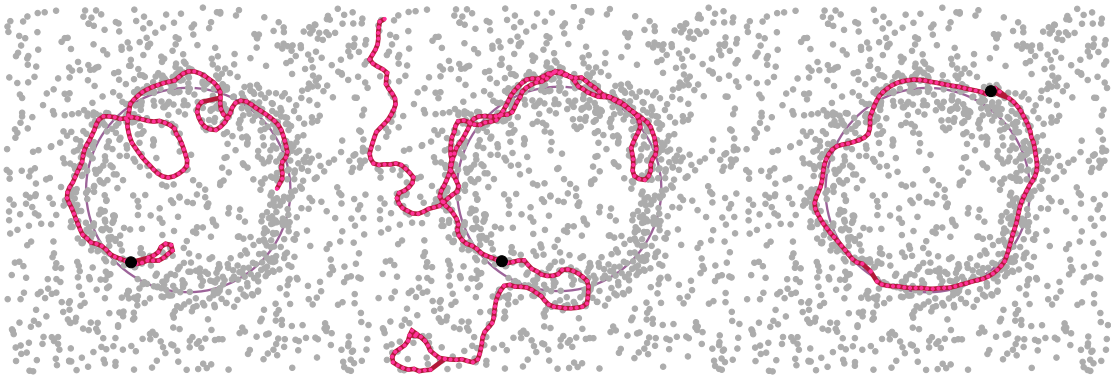

Figure 25: The reconstruction performance is improved in noisy data when employing a moving centroid in Equation (1); ($S_d = S_j = 1.0, N = 452, M = 904$). The Eigenvector direction becomes more robust. (Left to Right:) PDT, MN (PCA), and WMD.

Moreover, the centroid has an influence on the values of the multi-scale geometric measures. As mentioned in Section 5.1 – regarding $C_{L,max}$ of Equation (7) – employing the PDT improved the start point selection. For higher noise rates, starting points are favored in centers of point clusters. Figure 26 illustrates the first four starting point candidates for a noisy circle. When employing the PDT instead of a MN (PCA) or geometric median points are selected more closely to the ground truth geometry.

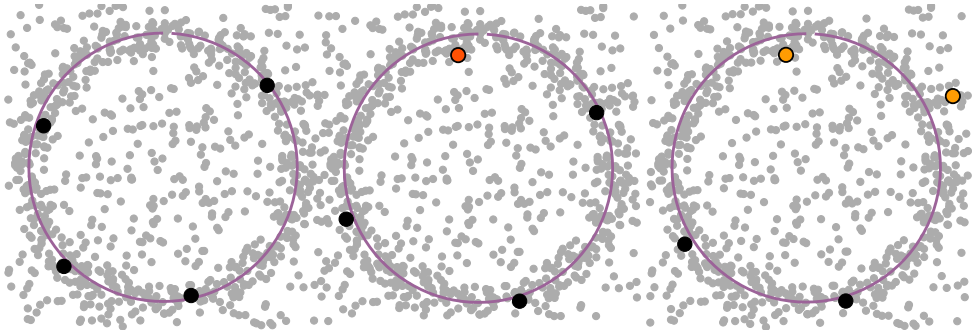

Figure 26: Influence of the centroid on selecting the start points. (Left to right): PDT, MN (PCA), and MD. For the PDT, the centroid remains fixed. Here, candidates in the center of noise clusters are scored better (left). By employing the median the starting point score of non optimal candidates is improved due to noise filtering (right).